Journal of Applied Ichthyology

J. Appl. Ichthyol. 26 (2010), 263–267

ISSN 0175–8659

Received: September 01, 2009
Accepted: December 29, 2009
doi: 10.1111/j.1439-0426.2010.01417.x

Canaliculi in the tessellated skeleton of cartilaginous fishes

By M. N. Dean[1,*], J. J. Socha[2], B. K. Hall[3,4] and A. P. Summers[1,5]

[1]*Ecology and Evolutionary Biology, University of California Irvine, Irvine, CA, USA;* [2]*Engineering Science and Mechanics, Virginia Tech, Blacksburg, VA, USA;* [3]*Department of Biology, Dalhousie University, Halifax, NS, Canada;* [4]*School of Life Sciences, Arizona State University, Tempe, AZ, USA;* [5]*Friday Harbor Labs, University of Washington, Friday Harbor, WA, USA*

Summary

The endoskeletal elements of sharks and rays are comprised of an uncalcified, hyaline cartilage-like core overlain by a thin fibro-ceramic layer of mineralized hexagonal tiles (tesserae) adjoined by intertesseral fibers. The basic spatial relationships of the constituent tissues (unmineralized cartilage, mineralized cartilage, fibrous tissue) are well-known – endoskeletal tessellation is a long-recognized synapomorphy of elasmobranch fishes – but a high-resolution and three-dimensional (3D) understanding of their interactions has been hampered by difficulties in sample preparation and lack of technologies adequate for visualizing microstructure and microassociations. We used cryo-electron microscopy and synchrotron radiation tomography to investigate tessellated skeleton ultrastructure but without damage to the delicate relationships between constituent tissues or to the tesserae themselves. The combination of these techniques allowed visualization of never before appreciated internal structures, namely passages connecting the lacunar spaces within tesserae. These intratesseral 'canaliculi' link consecutive lacunar spaces into long lacunar strings, radiating outward from the center of tesserae. The continuity of extracellular matrix throughout the canalicular network may explain how chondrocytes in tesserae remain vital despite encasement in mineral. Extracellular fluid exchange may also permit transmission of nutrients, and mechanical and mineralization signals among chondrocytes, in a manner similar to the canalicular network in bone. These co-adapted mechanisms for the facilitated exchange of extracellular material suggest a level of parallelism in early chondrocyte and osteocyte evolution.

Introduction

Mineralized biological materials such as shells and skeletons are composites, organized arrangements of an inorganic oxide phase (e.g. hydroxyapatite, calcium carbonate) and a biopolymer (e.g. collagen) (Chen et al., 2008; Fratzl and Weinkamer, 2007). The layered interaction of soft and hard materials is present in discrete patterns at all size scales, creating a complex hierarchy of inorganic/organic structures that determine the emergent mechanical properties of the tissue and also make morphological study difficult. Every size scale is characterized by a distinct and mechanically important structural pattern requiring consideration. However, yet the spatially complex interactions of the different material components mean that every imaging technique has drawbacks (e.g. in favoring one tissue type over others or overlooking the three-dimensionality of the tissue) (Fratzl and Weinkamer, 2007; Dean et al., 2009b).

The skeletal tissues of elasmobranch fishes (sharks, rays and relatives) illustrate the challenges of studying the hierarchical structure of biomaterials (Dean et al., 2009b). Nearly the entire skeleton is comprised of tessellated cartilage, in which uncalcified cartilage elements are sheathed, with a layer of abutting mineralized tiles (tesserae), joined together into a tiled mat by intertesseral collagen fibers (Clement, 1992; Dean and Summers, 2006; Kemp and Westrin, 1979; Summers, 2000) (Fig. 1A,B). Each tessera is a geometric block (hundreds of microns deep and wide in adults), comprised of hydroxyapatite crystals on a collagen scaffold (Applegate, 1967; Dean and Summers, 2006; Kemp and Westrin, 1979). The skeleton is therefore a fibro-mineral composite (perichondrium-tesserae-intertesseral fibers) wrapping a fiber-reinforced gel (uncalcified cartilage) with stark transitions between constituent tissues types (Dean et al., 2008, 2009b) (Fig. 1A,B).

Previous examinations of tessellated cartilage were hampered by methodologies that treat inorganic and organic components unequally and that limit three-dimensional understanding of tissue arrangements. For example, scanning electron microscopy (SEM) studies have largely focused on mineralized tissue (i.e. the tesserae themselves) at the expense of the soft tissues, in some cases, examining air-dried specimens or employing bleach protocols to remove organic phases (e.g. Applegate, 1967; Clement, 1992; Dingerkus et al., 1991; Kemp and Westrin, 1979). These techniques and critical point drying for SEM provide useful views of disarticulated tesserae but result in distortions in sample geometry from the shriveling and/or removal of unmineralized cartilage and fibrous (perichondrial, intertesseral) interactions. In addition, because tesserae are stiff, with complex interdigitations, cross-sectioning elasmobranch skeletal samples for traditional SEM can be damaging to the micromorphology of interest. Histological preparations for light microscopy can provide detailed soft tissue information, but lack the resolution and three-dimensional information of SEMs. Histology also usually requires decalcification (e.g. in EDTA or formic acid) to facilitate sectioning (e.g. Clement, 1992; Eames et al., 2007; Kemp and Westrin, 1979) which may alter morphologies native to the calcified phase.

An ideal tissue preparation technique for tessellated cartilage would preserve hard and soft tissue morphologies while allowing a three-dimensional understanding of tissue interactions. We achieve this here using low-temperature SEM

*Current address: Max Planck Institute for Colloids and Interfaces, Department of Biomaterials, D-14424 Potsdam, Germany.
E-mail: mason.dean@mpikg.mpg.de

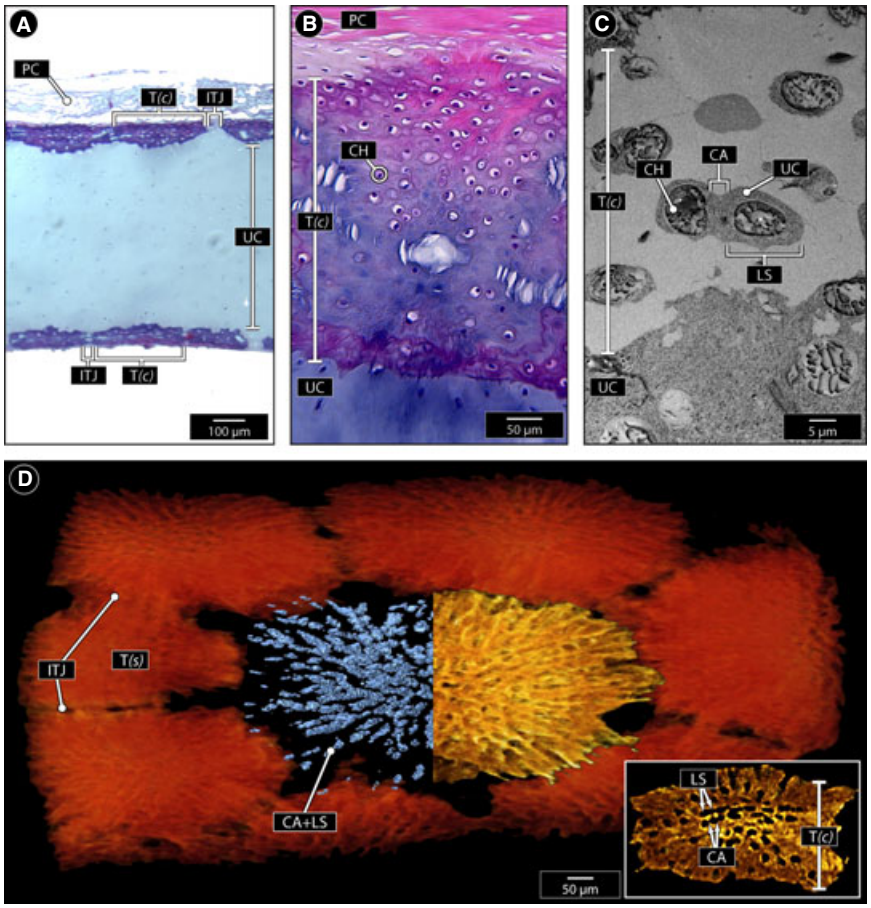

Fig. 1. The canalicular network in the tessellated skeleton of the round stingray, *Urobatis halleri*. Tessellated cartilage (panel a) is comprised of uncalcified cartilage (*UC*) surmounted by a mat of abutting mineralized blocks called tesserae (portions of several are shown in cross-section, *T(c)*, on the top and bottom surfaces of skeletal element), separated by intertesseral joints (*ITJ*) and overlain by a fibrous perichondrium (*PC*). Vital (non-necrotic) chondrocytes (*CH*; panel b) are found throughout uncalcified cartilage and intertesseral joints and also within tesserae themselves; in cryoSEM sections (panel c) cells are seen to be surrounded by a thin layer of unmineralized matrix (*UC*, appears in panel c as gray and porous material) and contained in mineralized lacunae (lacunar spaces, *LS*) connected to one another by short passageways (canaliculi, *CA*). These interconnected canaliculi and lacunar spaces (*CA* + *LS*) can be volume-rendered from synchrotron x-ray scans (panel d, showing a bisected tessera in surface aspect, *T(s)*, with half of its canalicular network visualized and surrounded by portions of seven neighboring tesserae) and appear to radiate outward from the center of each tessera toward its periphery. No organic material is visible in virtual sections of synchrotron x-ray data (panel d inset); lacunar spaces and connecting canaliculi appear as voids in the mineralized tissue. (Please see the online PDF for a color version of this figure)

(cryoSEM) and synchrotron radiation microcomputed tomography (SR-μCT) to examine the lower jaw cartilage of a stingray (*Urobatis halleri*). By combining these tools, the limitations of one technique (e.g. the two-dimensionality of SEM, the radio-transparency of soft tissues in x-rays) are accounted for by the other and we gain a high-resolution and tomographic understanding of the morphology of hydrated specimens. The morphological insight gained from our approach allows us to describe previously unknown structures, which we term intratesseral canaliculi; these small canals carry uncalcified extracellular matrix but apparently not cell processes between chondrocytes within tesserae.

Materials and methods

We examined tessellated cartilage from adult (> 150 mm disc width; the start of the adult size class for this species) Haller's round rays (*Urobatis halleri*); this species was chosen for its ease of acquisition, the tractable size of skeletal elements for our techniques, and because data exist on its skeletal ontogeny (Dean et al., 2009a). Stingrays used in this study were mortalities from beach seine collections in conjunction with age, growth and reproduction research at Seal Beach, California (Hale and Lowe, 2008; Mull et al., 2008). We dissected the jaws from specimens and froze them in elasmobranch Ringer's solution in test tubes until time of use, when they were rethawed in a water bath; the number of thawing events was reduced to avoid damage from ice crystallization (Szarko and Bertram, 2007, 2006). In dissection, the majority of muscle and tendinous tissue was cleaned away from the jaws. The thin perichondral envelope was left intact to avoid damage to the tessellated layer. The mid-shaft (parasymphyseal) region of the jaws was imaged in all cases.

The cryoSEM technique was developed for a previous study on tessellated cartilage ontogeny (Dean et al., 2009a) and is discussed in detail elsewhere (Dean et al., 2008). Briefly, samples were clamped in a cryo-stub and plunge-frozen in slushed liquid nitrogen, then cross-sectioned with a cold scalpel in a low-temperature (−140°C) preparation chamber; sectioning in this manner creates a smoother-faced section with fewer artifacts than would be possible at room temperature. The temperature in the sample chamber was raised to −95°C for 10–15 min to etch the sample, removing surface water and/or contaminants before sputter coating

with gold palladium (layer thickness: 6 nm). The sample was then introduced onto the SEM cryostage (Hitachi-4800, −120°C) and viewed at low accelerating voltages of 1–2 kV. This cryoSEM technique preserves *in situ* morphologies of hard (tesseral mineral) and soft (intertesseral fibers, chondrocytes, extracellular matrix) tissue phases, and therefore allows visualization of these skeletal components within tesserae. Morphological features of cross-sectioned tesserae were imaged digitally at 400× and 1000×. Two parasymphyseal, lower jaw (Meckel's cartilage) sections were observed for each of six adult individuals (152–213 mm disc width; the width of the body disc, rather than total length, is a common size-metric for rays).

Synchrotron micro-computed tomography (SRμ-CT) data were collected from the lower jaws of two adult specimens (225, 252 mm disc width) at the XOR-2BM beam line at the Advanced Photon Source (Argonne National Laboratory, Argonne, IL). As in conventional x-ray tomographic imaging, SRμ-CT allows samples to be visualized in three dimensions and virtually sectioned in any plane, but the higher photon flux and beam coherence of synchrotron imaging results in higher resolution imagery (with sub-micron detail, given adequate sample and detector size). To maintain hydration during sample imaging, we placed parasymphyseal jaw sections (approx. 0.5 cm wide and tall) in short segments cut from plastic drinking straws; these were filled with elasmobranch ringer solution, capped at both ends with clay, and mounted vertically on sample stubs. Samples were scanned with monochromatic x-rays (20 keV), using a sample-to-scintillator distance of 30 mm, 2.5× microscope objective, and a CoolSnapHQ camera (1024 × 1024 px). The field of view was 2.7 mm wide. The sample was rotated about the vertical axis, and 2D projection images were recorded every 1 / 8°. Three-dimensional volumes were reconstructed from projection images using custom software written for Advanced Photon Source scans, and images were output as 2D slices stacked vertically. The resulting resolution was approximately 1.3 μm (for further details on reconstruction techniques and custom software see Wang et al., 2001; Socha and De Carlo, 2008). Mandibular tesserae in adult *U. halleri* are approximately 300 μm (and up to nearly 500 μm) wide and approximately 200 μm deep (Dean et al., 2009a); our sample dimensions allowed for visualization of fields of at least 10 abutting tesserae per scan. The 2D slice images were volume-rendered using Amira software (v.5.2.1; Visage Imaging, San Diego, CA).

All constituent tissues in tessellated cartilage (unmineralized cartilage, mineralized cartilage, fibrous tissue) contain cells; these are presumed to be chondrocytes in both mineralized and unmineralized cartilage and interspersed among intertesseral fibers. Within tesserae, chondrocytes occupy 'lacunar spaces', holes in the mineralized tissue that make tesserae appear porous in histological cross-sections. Although previous authors refer to these as 'cell spaces' (e.g. Ørvig, 1951; Moss, 1968; Summers, 2000; Zangerl, 1966), we believe 'lacunar spaces' is more accurate because these chambers in tesserae contain cells and matrix. Our synchrotron x-ray scans allowed a three-dimensional view of only the hard tissue phase of tesserae, with within- and between- tesserae organic material (i.e. chondrocytes and intertesseral joints, respectively) appearing as empty spaces. The connectivity of within-tesserae spaces was visualized using the Selection Tool in the Label Field editor function of Amira, which allows for labeling and tracking of materials within a similar range of tissue density (image contrast).

Results

Intratesseral lacunar spaces are clearly visible using both methods. In cryoSEM sections, intratesseral chondrocytes are surrounded by a thin layer of pericellular matrix and then concentrically by mineralized tissue (Fig. 1C). Our synchrotron scans do not provide soft tissue information and so lacunar spaces appear as spheroidal voids in otherwise solid mineralized material (Fig. 1D, inset image). Small passages ('canaliculi') connect adjacent lacunar spaces end-to-end (Fig. 1C,D); although extracellular matrix is continuous through canaliculi, we saw no evidence of cellular processes extending into canaliculi from chondrocytes (Fig. 1C). The canalicular network – observed in three-dimensional reconstructions of synchrotron scans – joins many lacunar spaces in series, creating "lacunar strings" (chains of lacunae and canaliculi; Fig. 1D). Canaliculi are < 10 μm long and ≤ 5 μm in diameter, shorter than lacunar spaces in both dimensions (Fig. 1C); as a result, lacunar strings visualized in Amira appear as linear beaded necklaces (Fig. 1D). Lacunar strings appear to radiate outward from the center of tesserae in all directions, however the bulk of them run toward the intertesseral margins (where tesserae abut one another) (Fig. 1D).

Discussion

To the best of our knowledge, this is the first demonstration of intratesseral channels, although there appear to be multiple types of passages that perforate elasmobranch cartilage. Based on limited current knowledge, we feel these features of elasmobranch cartilages should be divided into two primary categories: cartilage canals and interlacunar 'canaliculi'. The term 'canaliculus' is typically reserved for description of passages through bone; a justification for our use of the term follows.

Cartilage canals, like those seen in mammalian cartilage, are large vascular passageways (hundreds of micrometers in diameter) that transport materials between perichondral regions and deep cartilage tissue (Blumer et al., 2004, 2008; Eslaminejad et al., 2006; Hall, 2005). Hoenig and Walsh (1982) observed these passages penetrating vertebral centra, the only elasmobranch endoskeletal tissues to exhibit areolar calcification, wherein mineralized tissue forms a web-like, mineralized scaffold in the chondrocyte-rich center of the vertebrae. Canals contained a variety of materials (chondrocytes, lymphatic and vascular tissues), were up to 350 μm in diameter, and were found only in those shark species that attain a large maximum size; the small shark and two batoid species examined lacked canals. It is likely that cartilage canals are found in other regions of the body: one of us (M.N. Dean, unpubl. data) has observed vascular canals, in gross dissections, extending beneath the teeth into the uncalcified cartilage of the tessellated lower jaw cartilage of blue sharks (*Prionace glauca*) and perforating the pectoral girdles of several batoid species. Whereas elasmobranch cartilage canals likely play a similar role to those of mammals in nourishing and maintaining cartilage, their association with deep uncalcified cartilage suggests that, unlike mammalian canals, they do not help to mediate mineralization (Hall, 2005).

In contrast, interlacunar canaliculi form communicating channels between adjacent lacunar spaces – mineralized lacunae containing chondrocytes and extracellular matrix – in areolar calcification (Clement, 1992; Ferreira and Vooren, 1991) and tesserae (tessellated cartilage; this study). 'Canalic-

ulus' is commonly used to describe short passages through plant and animal skeletal and digestive organs; but as this term is most associated with bone microstructure, we understand Clement's (1992) reluctance to apply it to elasmobranch cartilage structure. The canaliculi associated with osteocytes in bone are roughly an order of magnitude smaller in diameter and, in addition to extracellular fluids, carry the long cellular projections that allow osteocytes to maintain contact and signaling pathways within a mineralized matrix (Cowin, 1999; Burger and Klein-Nulend, 1999; Franz-Odendaal et al., 2006). Interlacunar passageways may simply be regions of overlap between the tips of the unmineralizing, extracellular domains of adjacent chondrocytes, as Clement (1992) seems to suggest. Although we saw no evidence of cellular processes adorning chondrocytes, we hypothesize that interlacunar canaliculi are functionally analogous to osteocyte canaliculi in allowing transport of material between lacunar spaces. Therefore we believe our nomenclature is consistent and appropriate.

The presence of interlacunar canaliculi may explain a long-standing paradox in elasmobranch skeletal biology wherein authors have noted that intratesseral chondrocytes appear vital, despite being encased in mineral (Egerbacher et al., 2006; Moss, 1968; Kemp and Westrin, 1979; Clement, 1992; Ferreira and Vooren, 1991; Dean et al., 2009a). Given our knowledge of the function of osteocytic canaliculi, elasmobranch canalicular networks suggest an open exchange of nutrients and communication among entombed cells and, in tesserae, perhaps among intra- and intertesseral chondrocytes. The continuity of extracellular matrix through intratesseral canaliculi is consistent with a system of extracellular fluid exchange, as seen around osteocytes, functioning to transduce finescale mechanical stresses and provide signals to guide mineral deposition (Burger and Klein-Nulend, 1999; Burger et al., 2003; Cowin, 1999). Cellular processes may exist in tessellated cartilage but were not observable with our methods; alternatively, it is also possible that elasmobranch chondrocytes did not evolve the mechanism to form gap junctions necessary for such intercellular communications or that fluid movement through the comparatively wide canaliculi provides adequate nutrient flow and a sufficiently strong signal for mechanotransduction.

Alkaline phosphatase activity has been demonstrated in regions of forming tesserae (Eames et al., 2007), but we know little of entombment signals and mechanisms in tessellated cartilage (e.g. whether cells entomb themselves or are buried by their neighbors). Ultrastructural examinations of tessellated cartilage suggest that tesserae thicken during ontogeny by engulfing arrays of chondrocytes from beneath them: cells in the underlying uncalcified cartilage organize into marginal rows and the mineralizing front appears to advance over them (Dean et al., 2009a; Kemp and Westrin, 1979). If every chondrocyte restricted the mineralization of the immediately surrounding matrix (Franz-Odendaal et al., 2006), this wholesale incorporation of multiple closely-associated cells would explain the presence of cell-rich laminae in tesserae and the observed morphology of lacunar strings.

Chondrocyte entombment was a feature of the earliest mineralized endoskeletons: lacunar spaces (and perhaps canaliculi; Zangerl, 1966 Fig. 24) in the calcified endoskeletal cartilage of extinct agnathans and basal gnathostomes (e.g. Janvier, 1997; Janvier and Arsenault, 2007; Moss, 1968; Zangerl, 1966; Ørvig, 1951), as well as induced *in vitro* calcification in lamprey cartilage (Langille and Hall, 1993) strongly suggest peri-chondrocytic mineralization is basal in craniates. Although not all vertebrate cartilages contain some type of perforating canal (Hall, 2005), our demonstration of interlacunar canaliculi in a basal gnathostome group points to pressures to maintain viable and communicating cells in a permanent, mineralized cartilage matrix. This facilitated exchange of extracellular matrix suggests that at least at this one level, chondrocytes and osteocytes, the two principal skeletogenic cells in vertebrates, exhibited parallelism in their early evolutionary pathways.

Our methods – which allow for a detailed three-dimensional understanding of the mineralized phase of the tessellated skeleton and, to a lesser degree, of its interaction with unmineralized phases – have revealed a canalicular network joining lacunar spaces within the mineralized phase of tessellated cartilage. Previous morphological examinations of tesserae have not noted canaliculi (Dingerkus et al., 1991; Kemp and Westrin, 1979) and some authors have asserted that they do not exist in tesserae (Shapiro, 1970; Clement, 1992). It is possible that the presence of canaliculi varies by species and/or location in the body, but living intratesseral chondrocytes observed across species suggest that previous two-dimensional methods were simply inadequate to visualize the canalicular network. Our discovery of these structures opens several avenues for research, as the phylogenetic occurrence, anatomical distribution, and histology of these canals surely have implications for elasmobranch cartilage mechanics, physiology and evolution.

Acknowledgements

We would like to thank the Workshop organizers for the invitation to present and for assembling a fascinating series of talks. We also thank Chris Lowe, Chris Mull, Lori Hale and the CSULB Shark Lab for unwavering generosity and specimens. The synchrotron work would not have been possible without the indefatigable Francesco de Carlo; Lena Gorb, Connie Miksch, Jan Schuppert, Matt Szarko and Dagmar Voigt were instrumental in developing and troubleshooting the cryoSEM technique. Use of the Advanced Photon Source was supported by the US. Department of Energy, Office of Science, Office of Basic Energy Sciences, under Contract No. DE-AC02-06CH11357. This research was supported by a National Science Foundation grant to MND and APS (IOB-0616322) and a Josephine de Kármán Fellowship to MND; attendance at the Workshop was funded by a Company of Biologists Direct Travel Grant.

References

Applegate, S. P., 1967: A survey of shark hard parts. In Sharks, skates and rays. P. W. Gilbert, R. F. Mathewson, D. P. Rall (Eds). Johns Hopkins Press, Maryland, pp. 37–66.

Blumer, M. J. F.; Fritsch, H.; Pfaller, K.; Brenner, E., 2004: Cartilage canals in the chicken embryo: ultrastructure and function. Anat. Embryol. **207,** 453–462.

Blumer, M. J. F.; Longato, S.; Fritsch, H., 2008: Structure, formation and role of cartilage canals in the developing bone. Ann. Anat. **190,** 305–315.

Burger, E. H.; Klein-Nulend, J., 1999: Mechanotransduction in bone – role of the lacuno-canalicular network. FASEB J. **13,** S101–S112.

Burger, E. H.; Klein-Nulend, J.; Smit, T. H., 2003: Strain-derived canalicular fluid flow regulates osteoclast activity in a remodelling osteon – a proposal. J. Biomech. **36,** 1453–1459.

Chen, P.-Y.; Lin, A. Y. M.; Lin, Y.-S.; Seki, Y.; Stokes, A. G.; Peyras, J.; Olevsky, E. A.; Meyers, M. A.; McKittrick, J., 2008: Structure and mechanical properties of selected biological materials. J. Mech. Behav. Biomed. Mater. **1,** 208–226.

Clement, J. G., 1992: Re-examination of the fine structure of endoskeletal mineralization in Chondrichthyes: implications for growth, ageing and calcium homeostasis. Aust. J. Mar. Freshw. Res. **43,** 157–181.

Cowin, S. C., 1999: Bone poroelasticity. J. Biomech. **32,** 217–238.

Dean, M. N.; Summers, A. P., 2006: Cartilage in the skeleton of cartilaginous fishes. Zoology **109,** 164–168.

Dean, M. N.; Gorb, S. N.; Summers, A. P., 2008: A cryoSEM method for preservation and visualization of calcified shark cartilage (and other stubborn heterogeneous skeletal tissues). Micros. Today **16,** 48–50.

Dean, M. N.; Hale, L. F.; Mull, C. G.; Gorb, S. N.; Summers, A. P., 2009a: Ontogeny of the tessellated skeleton: insight from the skeletal growth of the round stingray *Urobatis halleri*. J. Anat. **215,** 227–239.

Dean, M. N.; Swanson, B. O.; Summers, A. P., 2009b: Biomaterials: properties, variation and evolution. Int. Comp. Biol. **49,** 15–20.

Dingerkus, G.; Séret, B.; Guilbert, E., 1991: Multiple prismatic calcium phosphate layers in the jaws of present-day sharks (Chondrichthyes; Selachii). Experientia **47,** 38–40.

Eames, B. F.; Allen, N.; Young, J.; Kaplan, A.; Helms, J. A.; Schneider, R. A., 2007: Skeletogenesis in the swell shark *Cephaloscyllium ventriosum*. J. Anat. **210,** 542–554.

Egerbacher, M.; Helmreich, M.; Mayrhofer, E.; Böck, P., 2006: Mineralisation of the hyaline cartilage in the small-spotted dogfish *Scyliorhinus canicula* L. Scr. Med. (BRNO) **79,** 199–212.

Eslaminejad, M. R. B.; Valojerdi, M. R.; Yazdi, P. E., 2006: Computerized three-dimensional reconstruction of cartilage canals in chick tibial chondroepiphysis. Anat. Histol. Embryol. **35,** 247–252.

Ferreira, B. P.; Vooren, C. M., 1991: Age, growth, and structure of vertebra in the school shark *Galeorhinus galeus* (Linnaeus, 1758) from southern Brazil. Fish. B-NOAA. **89,** 19–31.

Franz-Odendaal, T. A.; Hall, B. K.; Witten, P. E., 2006: Buried alive: how osteoblasts become osteocytes. Dev. Dyn. **235,** 176–190.

Fratzl, P.; Weinkamer, R., 2007: Nature's hierarchical materials. Prog. Mater. Sci. **52,** 1263–1334.

Hale, L. F.; Lowe, C. G., 2008: Age and growth of the round stingray, *Urobatis halleri* at Seal Beach, California. J. Fish Biol. **73,** 510–523.

Hall, B. K., 2005: Bones and cartilage: developmental skeletal biology. Elsevier / Academic Press, London, 792 pp.; ISBN: 0123190606.

Hoenig, J. M.; Walsh, A. H., 1982: The occurrence of cartilage canals in shark vertebrae. Can. J. Zool. **60,** 483–485.

Janvier, P., 1997: Early vertebrates. Oxford University Press, Oxford, UK, 408 pp.; ISBN: 0198540477.

Janvier, P.; Arsenault, M., 2007: The anatomy of *Euphanerops longaevus* Woodward, 1900, an anaspid-like jawless vertebrate from the Upper Devonian of Miguasha, Quebec, Canada. Geodiversitas **29,** 143–216.

Kemp, N. E.; Westrin, S. K., 1979: Ultrastructure of calcified cartilage in the endoskeletal tesserae of sharks. J. Morphol. **160,** 75–102.

Langille, R. M.; Hall, B. K., 1993: Calcification of cartilage from the lamprey *Petromyzon marinus* (L) in vitro. Acta Zool. **74,** 31–41.

Moss, M., 1968: The origin of vertebrate calcified tissues. In: Current problems of lower vertebrate phylogeny. T. Ørvig (Ed.). Almqvist and Wiksell, Stockholm, pp. 373–397.

Mull, C. G.; Lowe, C. G.; Young, K. A., 2008: Photoperiod and water temperature regulation of seasonal reproduction in male round stingrays (*Urobatis halleri*). Comp. Biochem. Physiol. A Physiol. **151,** 717–725.

Ørvig, T., 1951: Histologic studies of placoderms and fossil elasmobranchs. I: the endoskeleton, with remarks on the hard tissues of lower vertebrates in general. Arkiv. Zool. **2,** 321–454.

Shapiro, I. M., 1970: Phospholipids of mineralized tissues .2. Elasmobranch and teleost skeletal tissues. Calcif. Tissue Res. **5,** 30–38.

Socha, J. J.; De Carlo, F., 2008: Use of synchrotron tomography to image naturalistic anatomy in insects. In: Developments in x-ray tomography VI. SPIE, San Diego, CA: pp. 70780A–70787A.

Summers, A. P., 2000: Stiffening the stingray skeleton – An investigation of durophagy in myliobatid stingrays (Chondrichthyes, Batoidea, Myliobatidae). J. Morphol. **243,** 113–126.

Szarko, M. J.; Bertram, J. E. A., 2006: Freeze-thaw treatment alters articular cartilage dynamic behaviour. Int. Comp. Biol. **46,** E139.

Szarko, M.; Bertram, J. E. A., 2007: Articular cartilage function and organization: integrating dynamic mechanics with cryopreservation effects. J. Morphol. **268,** 1140.

Wang, Y. X.; De Carlo, F.; Mancini, D. C.; McNulty, I.; Tieman, B.; Bresnahan, J.; Foster, I.; Insley, J.; Lane, P.; von Laszewski, G.; Kesselman, C.; Su, M. H.; Thiebaux, M., 2001: A high-throughput x-ray microtomography system at the Advanced Photon Source. Rev. Sci. Instrum. **72,** 2062–2068.

Zangerl, R., 1966: A new shark of the family Edestidae, *Ornithoprion hertwigi* from the Pennsylvanian Mecca and Logan quarry shales of Indiana. Fieldiana Geol. **16,** 1–43.

Author's address: Mason Dean, Max Planck Institute for Colloids and Interfaces, Department of Biomaterials, D-14424 Potsdam, Germany.
E-mail: mason.dean@mpikg.mpg.de